General Disclaimer

One or more of the Following Statements may affect this Document

- This document has been reproduced from the best copy furnished by the organizational source. It is being released in the interest of making available as much information as possible.

- This document may contain data, which exceeds the sheet parameters. It was furnished in this condition by the organizational source and is the best copy available.

- This document may contain tone-on-tone or color graphs, charts and/or pictures, which have been reproduced in black and white.

- This document is paginated as submitted by the original source.

- Portions of this document are not fully legible due to the historical nature of some of the material. However, it is the best reproduction available from the original submission.

Produced by the NASA Center for Aerospace Information (CASI)

EXPLOSIVE HYPERVELOCITY DRAG ACCELERATOR

PIFR-269

by

M. B. Gross

May 1971

Prepared for
National Aeronautics and Space Administration
Manned Spacecraft Center
Houston, Texas 77058

Under Contract No. NAS-9-11083

N71-29227
(ACCESSION NUMBER) (THRU)
43 G3
(PAGES) (CODE)
CR-115067 11
(NASA CR OR TMX OR AD NUMBER) (CATEGORY)
FACILITY FORM 602

JUL 1971
RECEIVED
NASA STI FACILITY
INPUT BRANCH

PHYSICS INTERNATIONAL COMPANY
2700 MERCED STREET • SAN LEANDRO, CALIFORNIA 94577 • PHONE 357-4610 (415) • TWX 891-9689 (415)

CR-115067

EXPLOSIVE HYPERVELOCITY DRAG ACCELERATOR

PIFR-269

by

M. B. Gross

May 1971

Prepared for

National Aeronautics and Space Administration
Manned Spacecraft Center
Houston, Texas 77058

Under Contract No. NAS-9-11083

Prepared by

Physics International Company
2700 Merced Street
San Leandro, California 94577

ABSTRACT

This report presents the results of a program to evaluate the basic operating parameters of an explosive hypervelocity drag accelerator. The drag accelerator is an explosive charge which produces a high-velocity jet of gaseous explosive products. Projectiles are launched by the drag forces of the jet. Variables studied included projectile position in relation to the charge, projectile material, type of explosive, and ambient gas within the charge bore. The growth of the boundary layer and the uniformity of the jet were also investigated. The maximum projectile velocity attained during the program was 10.0 km/sec with a steel sphere 1.6 mm in diameter.

FOREWORD

This report was prepared by Physics International Company, San Leandro, California, under contract No. NAS-9-11083 and was funded by the NASA Manned Spacecraft Center, Houston, Texas. Mr. Burton G. Cour-Palais acted as contract monitor. The project supervisor and manager for Physics International were Dr. Stephen P. Gill and Mr. Michael B. Gross, respectively.

CONTENTS

ILLUSTRATIONS

SECTION 1
INTRODUCTION

Since 1961 the Soviet Union has been actively pursuing the development of hypervelocity launchers which use the drag forces of explosive jets to launch projectiles. In recent literature, Titov and Fadayenko (References 1 and 2) have reported achieving velocities of up to 14 km/sec with steel, ceramic, and glass spheres 0.1 to 10 mm in diameter. Using an apparently similar device, Rusakov (References 3 and 4) has attained 25 km/sec with a 0.2-gram cluster of tungsten microparticles.

The capability of reproducing the Russian results is desirable for two reasons: first, the Russian drag accelerator is a proven technique for launching spheres to velocities of 14 km/sec and would be immediately useful as a ground test facility for the study of hypervelocity meteorite impact on spacecraft structures; second, the device is lightweight and simple to operate. It can be launched to high altitudes by a booster rocket and fired into the atmosphere to generate an artificial meteorite of known mass and velocity. Optical data obtained from the artificial meteorite can then be used to interpret meteorite observation records in order to determine mass, velocity, and impact frequency statistics. The goal of this program was to investigate the basic operating parameters of the explosive drag accelerator and to try to duplicate the Russian achievement of a 14 km/sec projectile.

Section 2 presents a theoretical analysis of the explosive drag accelerator. A discussion of the experimental results of this program is presented in Section 3. Finally, Section 4 gives the conclusions and recommendations of this program.

SECTION 2
THEORETICAL ANALYSIS OF THE EXPLOSIVE DRAG ACCELERATOR

The explosive drag accelerator is based on the concept of the "cumulative charge" developed by Soviet Academician M. A. Lavrentyev (References 5 and 6). A cumulative charge is a thick-walled cylinder of explosive. When a detonation wave propagates axially down the charge, the high pressures behind the detonation cause gaseous explosive products to be imploded radially toward the charge axis (see Figure 1). Under the proper conditions, which for a hollow cylinder of explosive implies having a sufficiently large outer-diameter-to-inner-diameter ratio, a jet of explosive products will shoot forward from the point of convergence. An exact analysis of the compressible jetting flow is extremely complex, involving expansion behind the detonation wave, turning of the flow, and reexpansion to fill the inner diameter of the charge while driving a shock into the ambient gas within the charge. An analytical solution for the axially symmetric, compressible jet has not been found; therefore, an approximate, one-dimensional theory based on the integral conservation laws of mass, energy, and momentum will be described in Section 2.1.

2.1 PERFECTLY CONFINED CUMULATIVE CHARGE

The case of a perfectly confined cumulative charge is the simplest to consider, because all flow is in the axial direction. The more realistic case of imperfect confinement requires a considerably more sophisticated treatment. The basic concepts are

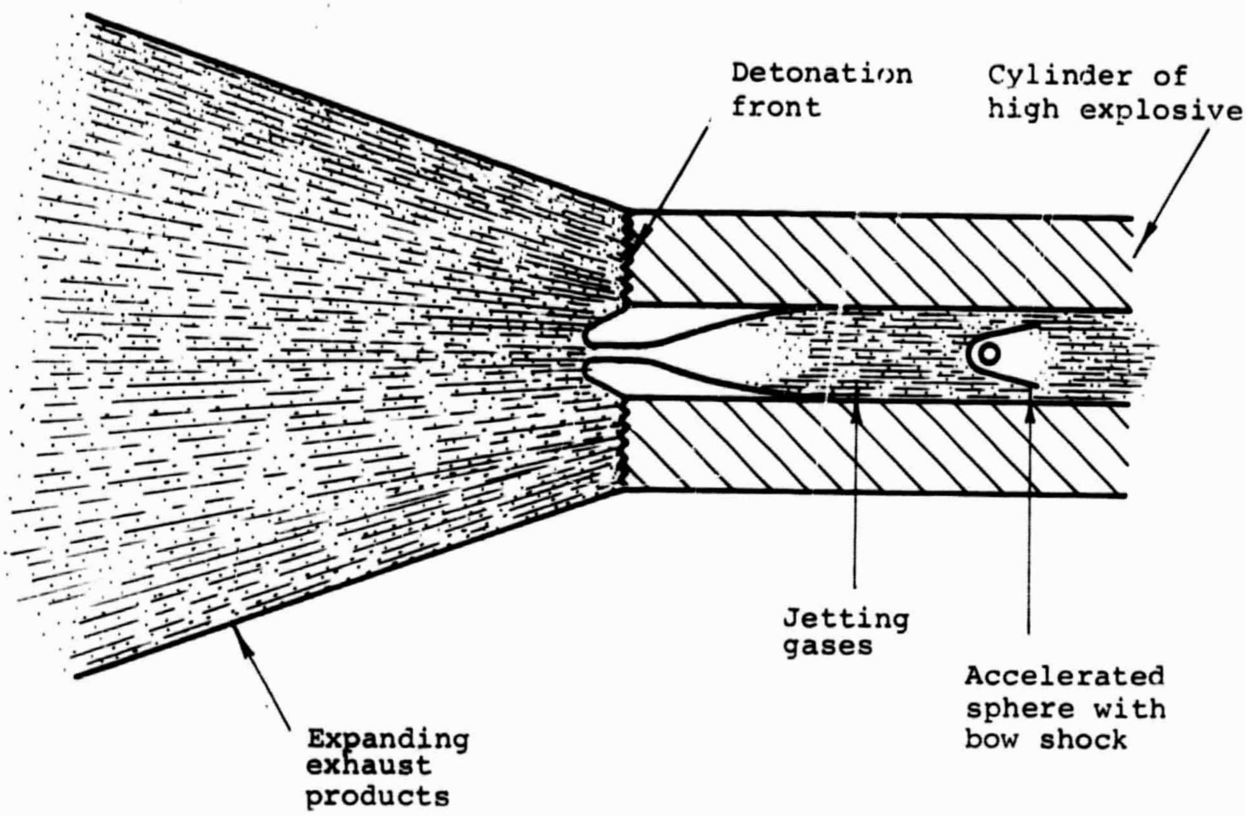

Figure 1   Schematic of cumulative charge drag accelerator.

8497

similar, however, so that calculations of the perfectly confined charge provide the basis for subsequent refinements. In addition, perfect confinement is the most efficient explosive configuration and represents an upper bound on accelerator performance.

Consider the case of a steady-state detonation in a perfectly confined cumulative charge (see Figure 2). At sufficiently large distances from the detonation and jet formation region, the jet and exhaust gases have uniform properties at an axial cross section. The integral conservation laws may be applied to a control surface across the flow at these points.

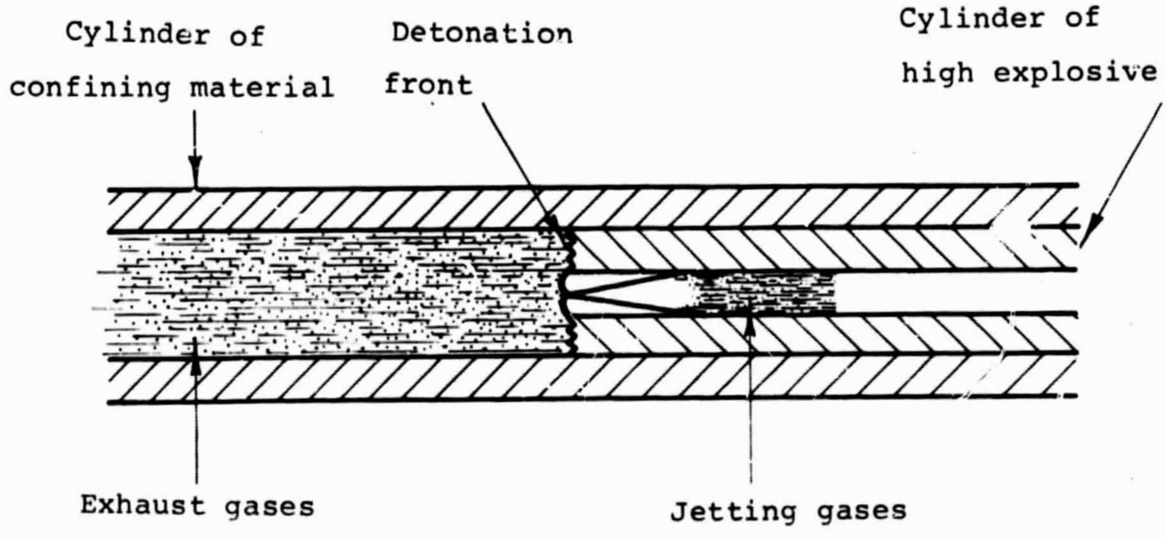

Figure 2 Perfectly confined cumulative charge.

Let the explosive charge mass per unit length be C, the detonation velocity D, the cross-sectional area of the jet stream A_j, the area of the exhaust stream A_e, density ρ, pressure p, enthalpy h, and velocity u. Then in the steady-state frame of reference we have:

Conservation of Mass:

$$CD = \rho_j u_j A_j + \rho_e u_e A_e \tag{1}$$

Conservation of Axial Momentum:

$$CD^2 + p_j A_j - p_e A_e = \rho_e u_e^2 A_e - \rho_j u_j^2 A_e \tag{2}$$

For any stream tube in steady-state flow, the first law of thermodynamics implies that

$$h + \frac{1}{2} u^2$$

is a constant. Choosing a stream tube in the jet and a stream tube in the exhaust:

$$h_j + \frac{1}{2} u_j^2 = E + \frac{1}{2} D^2 \tag{3}$$

$$h_e + \frac{1}{2} u_e^2 = E + \frac{1}{2} D^2 \tag{4}$$

where E is the internal energy per unit mass of the explosive. Finally an arbitrary equation of state may be assumed:

$$h = f(p, \rho) \tag{5}$$

Equations (1) through (5) reduce to four equations in the six unknowns p_j, u_j, ρ_j, p_e, u_e, ρ_e. For a unique solution, it is necessary to obtain two more equations, which can be shown to be equivalent to identifying the entropy of the exhaust and jet gases. Thus the flow variables can be calculated if the entropy generated in the gas expansion and jetting can be estimated, because the detonation entropy of the explosive is known.

Rather than attempt to estimate the entropy, it will be further assumed that the jet and exhaust gases are highly expanded, i.e., $p_e \cong p_j \cong 0$. The equations become exactly soluble, yielding

$$u_e = u_j = D\sqrt{1 + \frac{2E}{D^2}} \tag{6}$$

$$\rho_e = \frac{C}{2A_e} \, \frac{\sqrt{1 + \frac{2E}{D^2}} + 1}{1 + \frac{2E}{D^2}} \tag{7}$$

and

$$\rho_j = \frac{C}{2A_j} \, \frac{\sqrt{1 + \frac{2E}{D^2}} - 1}{1 + \frac{2E}{D^2}} \tag{8}$$

In particular, the jet velocity in the laboratory frame of reference is found to be:

$$u_j' = u_j + D = D\left(1 + \sqrt{1 + \frac{2E}{D^2}}\right) \tag{9}$$

For most explosives, $\frac{2E}{D^2} \cong 0.15$ is an excellent approximation, and the predicted jet velocity is found to be slightly greater than twice the detonation velocity.

The flow velocity for the highly expanded jet can be most closely compared to a charge fired in a vacuum. Titov and Fadeyenko (Reference 2) have reported a jet-driven air shock velocity in 1-torr air of 18.1 km/sec, corresponding to a particle velocity of 16.6 km/sec. The Russian explosive had a detonation velocity of 7.6 km/sec. Assuming that $\frac{2E}{D^2} \cong 0.15$, then the predicted jet velocity is

$$u_j' = 2.08 \ D = 15.8 \text{ km/sec}$$

The small difference between 15.8 and 16.6 can be explained by the unsteady expansion necessary to match the steady-state jet conditions to the low-pressure air shock Hugoniot.

2.2 CONSTANT DRAG ACCELERATION

The trajectory of a drag-accelerated spherical projectile can be readily calculated if the drag coefficient and free-stream jet properties are assumed to be constant. Equating the acceleration of the projectile to the drag force,

$$m \frac{dw}{dt} = \frac{1}{2} C_d A \rho_j (u_j - w)^2 \tag{1}$$

Here m is the projectile mass, C_d the drag coefficient, A the projectile cross-sectional area, ρ_j the jet density, u_j the jet velocity, and w the projectile velocity. The parameter k is defined by

$$k \equiv \frac{1}{2} \frac{C_d A \rho_j}{m} = \frac{3}{4} \frac{C_d \rho_j}{d_b \rho_b} \tag{2}$$

where d_b is the projectile diameter, and ρ_b the projectile density. Then

$$\frac{dw}{dt} = k\,(u_j - w)^2 \tag{3}$$

Integrating this equation,

$$\frac{w}{u_j} = \frac{ktu_j}{ktu_j + 1} \tag{4}$$

and

$$kx = ktu_j - \ell n\,(ktu_j + 1) \tag{5}$$

Given a terminal projectile velocity and an acceleration distance x, the above equations may be used to calculate the average jet density ρ_j. Assume the jet velocity is twice the detonation velocity; then the value of ktu_j can be calculated from Equation (4), and kx and k are known from Equation (5). The drag coefficient of a sphere in hypersonic flow is 0.91 (see Reference 2), and Equation (2) may be solved for ρ_j, using the initial diameter and density of the projectile. Typical densities calculated in this fashion were approximately 0.06 grams/cc, which compares well to the Russian average density of 0.0605 grams/cc.

SECTION 3
EXPERIMENTAL RESULTS

Extensive experiments with an explosive drag accelerator were conducted by Physics International Company under NASA sponsorship. Parameters and variables studied were the distance from the projectile to the detonation end of the explosive charge (run-in distance), distance from the projectile location to the charge muzzle (acceleration path), projectile material, projectile suspension system, boundary layer growth, uniformity of the jet, ambient gas in the charge bore, explosive geometry, and type of explosive. Typically, experiments were instrumented with flash radiographs, shorting range switches, and a high-speed framing camera on the range. Shorting ionization pins monitored the performance of the explosive. The explosive used for the majority of the tests was Detatube, Type 1, manufactured by E. I. duPont de Nemours and Company. Detatube is an extruded charge, made from an explosive material designated EL506-C, with nominal dimensions of 5/8-inch inner diameter and 1-3/4-inch outer diameter and a detonation velocity of 7.1 km/sec.

Prior to this program, a preliminary drag accelerator test shot was fired with in-house funding. The design parameters for this shot were given to Dr. S. P. Gill of Physics International by the Russian scientists investigating the drag accelerator while Dr. Gill was visiting Novosibirsk, USSR. The shot successfully launched a 1.6-mm steel sphere to 6.7 km/sec.

A table summarizing the results of this program is presented in subsection 3.6. Appendix A contains a table listing the shots fired, their purpose, and the specific instrumentation on each shot.

3.1 EXPERIMENTS 1.1 AND 1.2

The first experiments investigated two basic approaches that could be used during the program. The first approach was to change from a cylindrical to a rectangular explosive geometry (shot 1.1) while the second method was to fire the charges in a vacuum to improve performance (shot 1.2).

The rectangular driver appeared to have several advantages over the cylindrical charge. The jet of a rectangular charge theoretically has higher performance than the jet of a cylindrical charge because the convergence effect at the cylinder's axis will produce a more violent, i.e., a more irreversible, turning of the flow. Therefore, the planar geometry should generate less entropy in turning the flow and have less degradation of the jet than the cylindrical case. In addition, rectangular drivers with a wide variation of C/A_j (charge mass per unit length to jet area ratio) can easily be built with Detasheet (slabs of EL506-C explosive). Detatube, which was the explosive charge used for the majority of the shots, is available in only two sizes.

The results of shot 1.1 indicated that the rectangular charge did not launch any projectiles. A study of the high-speed framing camera record demonstrated that the explosive charge did not jet. Post-shot analysis of the gasdynamics of the jetting process indicated that using a thicker explosive layer would solve this problem.

Shot 1.2 was a close repetition of the preliminary experiment, the major difference being that, on the second shot, the ambient gas in the charge bore was air at 12-mm pressure. It was thought that the low-pressure atmosphere might improve performance by reducing the counter-pressure on the projectile. Also, the results of the Russian investigations (see Reference 2) showed that low pressures were effective in eliminating boundary layer effects from typical charge lengths used during the program. Since boundary layer degradation reduces the velocity of the jetting gases, projectile velocity might be increased if these effects were absent.

No projectile was detected on the instrumentation for shot 1.2, which consisted of flash radiographs, range switches, and a target. The most probable cause of failure was a large angular divergence of the projectile, with either the projectile impacting on the Lucite walls of the vacuum system and destroying itself or diverging from the main jet stream and not accelerating quickly enough to avoid being overtaken by the detonation wave. The possibility of the latter occurring is supported by calculations which demonstrate that a projectile launched in a vacuum accelerates slower than a projectile launched in atmospheric air. In the preliminary experiment (fired in atmospheric air) the sphere emerged just ahead of the detonation front.

At this point in the program, it was decided to return to experimenting with the basic, drag accelerator design of a cylindrical charge fired in ambient air. It was felt that further development of the rectangular geometry or the use of a low-pressure atmosphere could be most effectively investigated later in the program.

3.2 EXPERIMENTS 1.3 THROUGH 1.10 - VARIATION OF PROJECTILE MATERIAL AND POSITION

Experiments 1.3 through 1.10 focused on finding an acceptable projectile material and on the effect of varying the run-in distance and the acceleration path length. All experiments used Detatube and all projectiles were 1.6-mm- (1/16 inch-) diameter spheres placed on the charge axis. Material for projectiles during the program was annealed 52100 steel, hardened 52100 steel, and hardened 410 stainless steel. The 410 stainless steel sphere broke up when tested in an accelerator. Both forms of 52100 steel were acceptable for projectiles, but the annealed spheres were used because of their better quality control and availability.

Variation of the run-in distance and acceleration path length demonstrated that the projectile velocity depended on both these parameters and also on the angular divergence. Run-in distances were 32 cm and 40 cm while acceleration paths of 4, 8, and 12 cm were used. A typical experiment in this series is shot 1.7, which had a run-in of 32 cm and an acceleration path of 8 cm. Figure 3 shows the experimental set-up with the explosive charge in place. Two range switches and one of the two X-ray film cassettes can be seen in the picture. The mirror above the near portion of the range allows this region of the shot to be photographed by the high-speed framing camera. A distance-time plot of this shot is shown in Figure 4. The projectile velocity between the position on the first flash radiograph and the first range switch is 6.95 km/sec. From this flash radiograph (Figure 5) it may be seen that the soft annealed 52100 steel sphere has been flattened during the launch cycle. For comparison, a set-up projectile may be seen just above the saw blade at the bottom of the picture. Finally, the projectile drilled through the 1/4-inch-thick aluminum target at the end of the range (Figure 6).

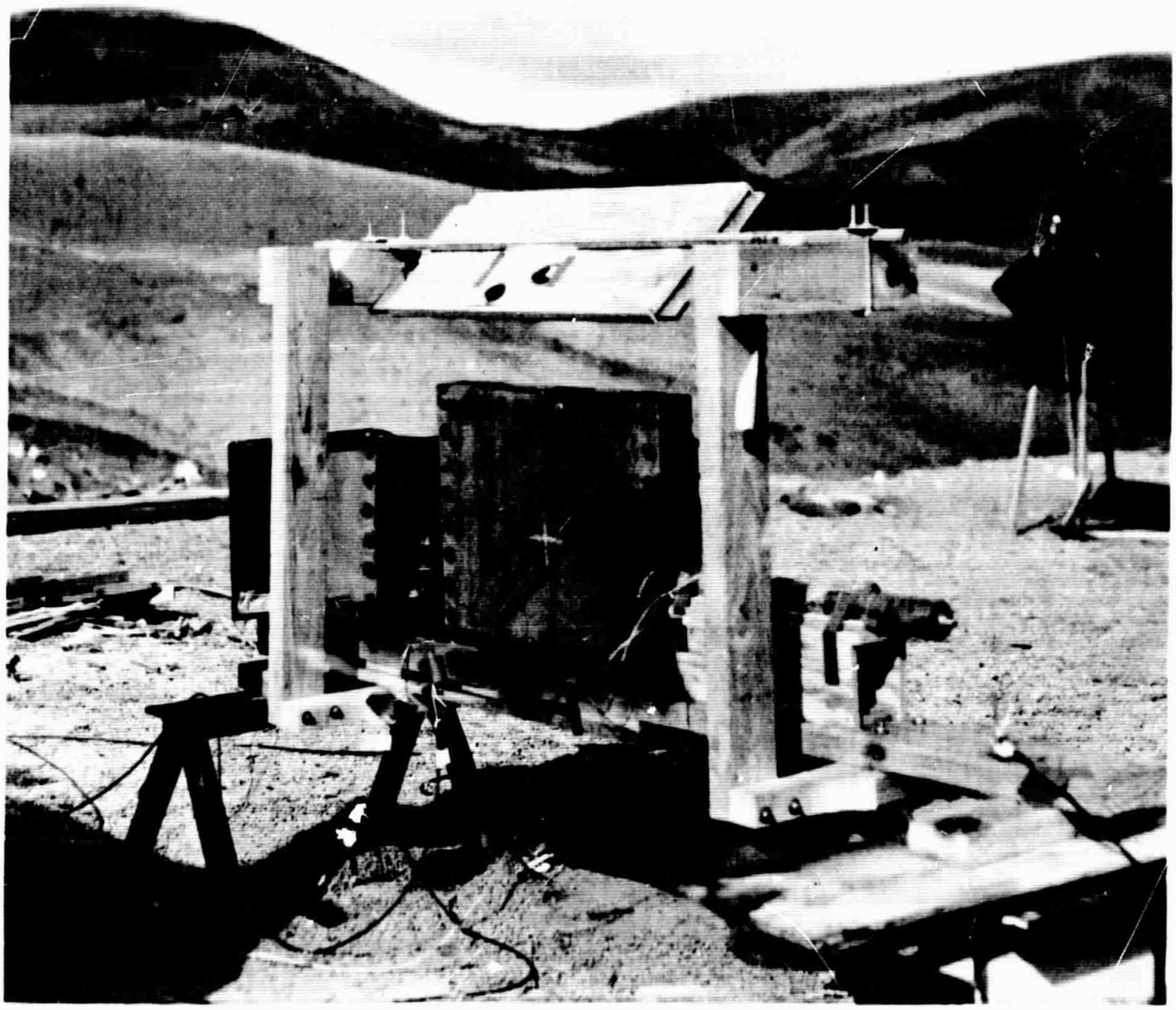

Figure 3 Pre-shot experimental set-up for shot 1.7.

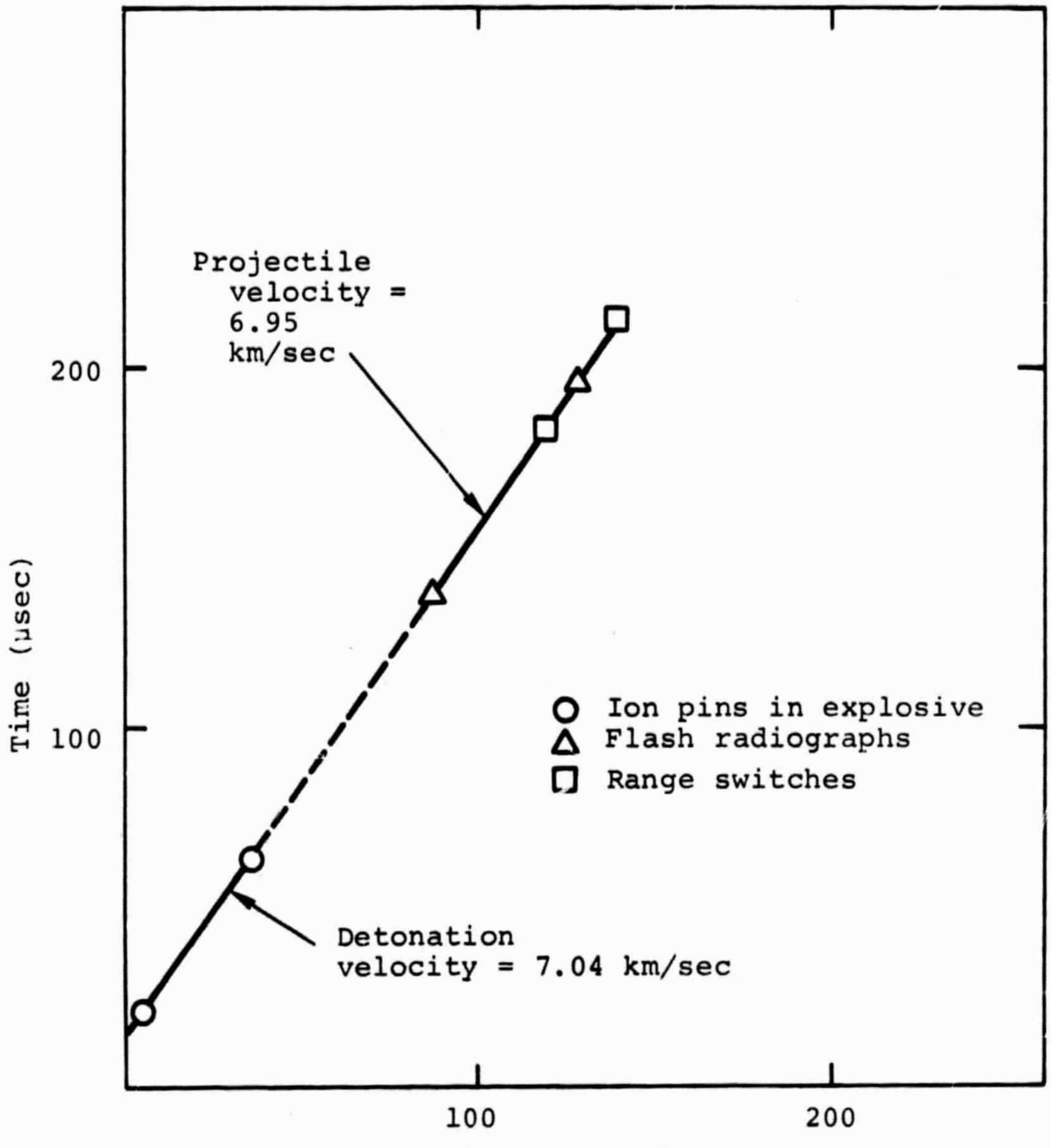

Figure 4 Distance - time plot for shot 1.7.

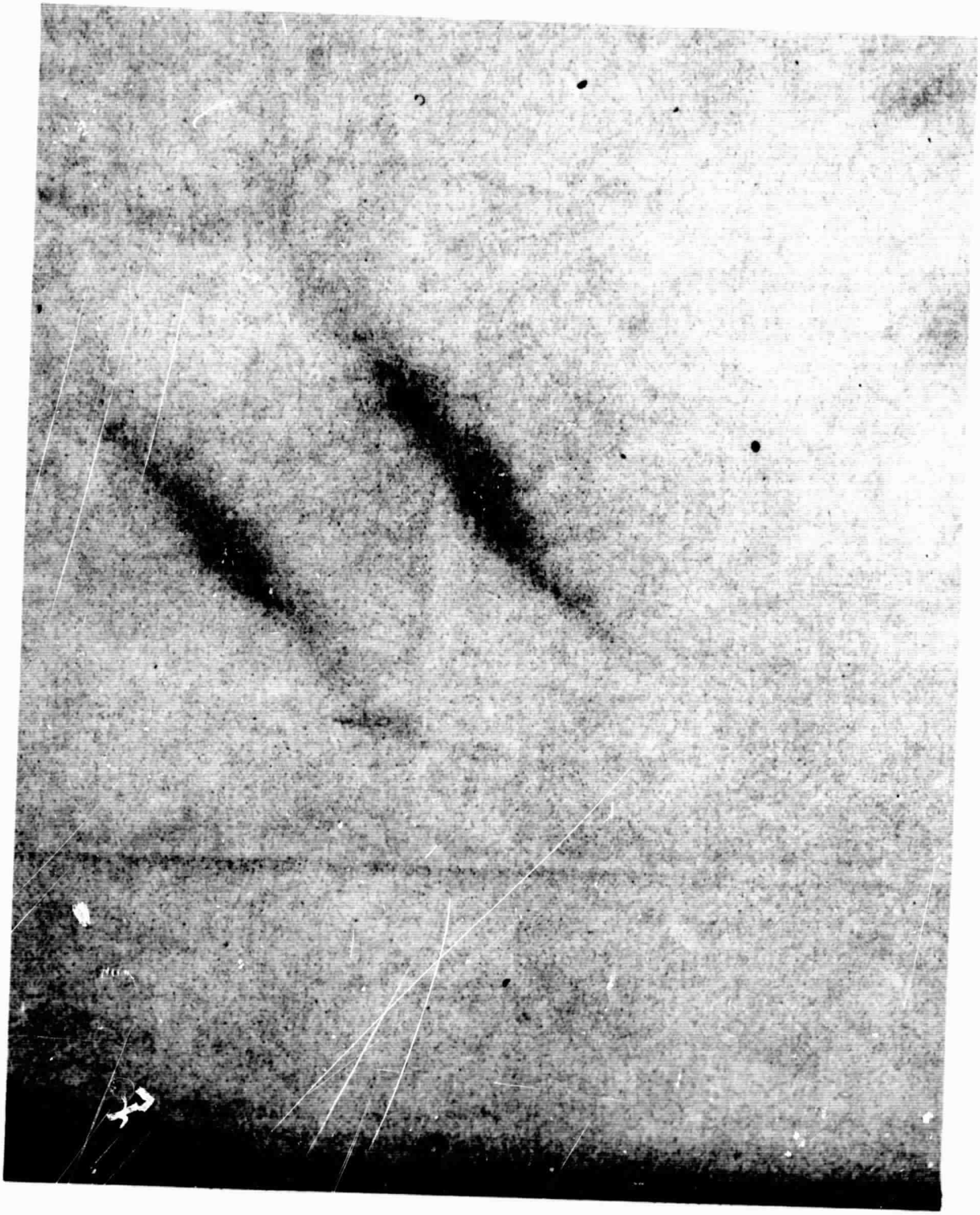

Figure 5 Flash radiograph, first cassette, shot 1.7.

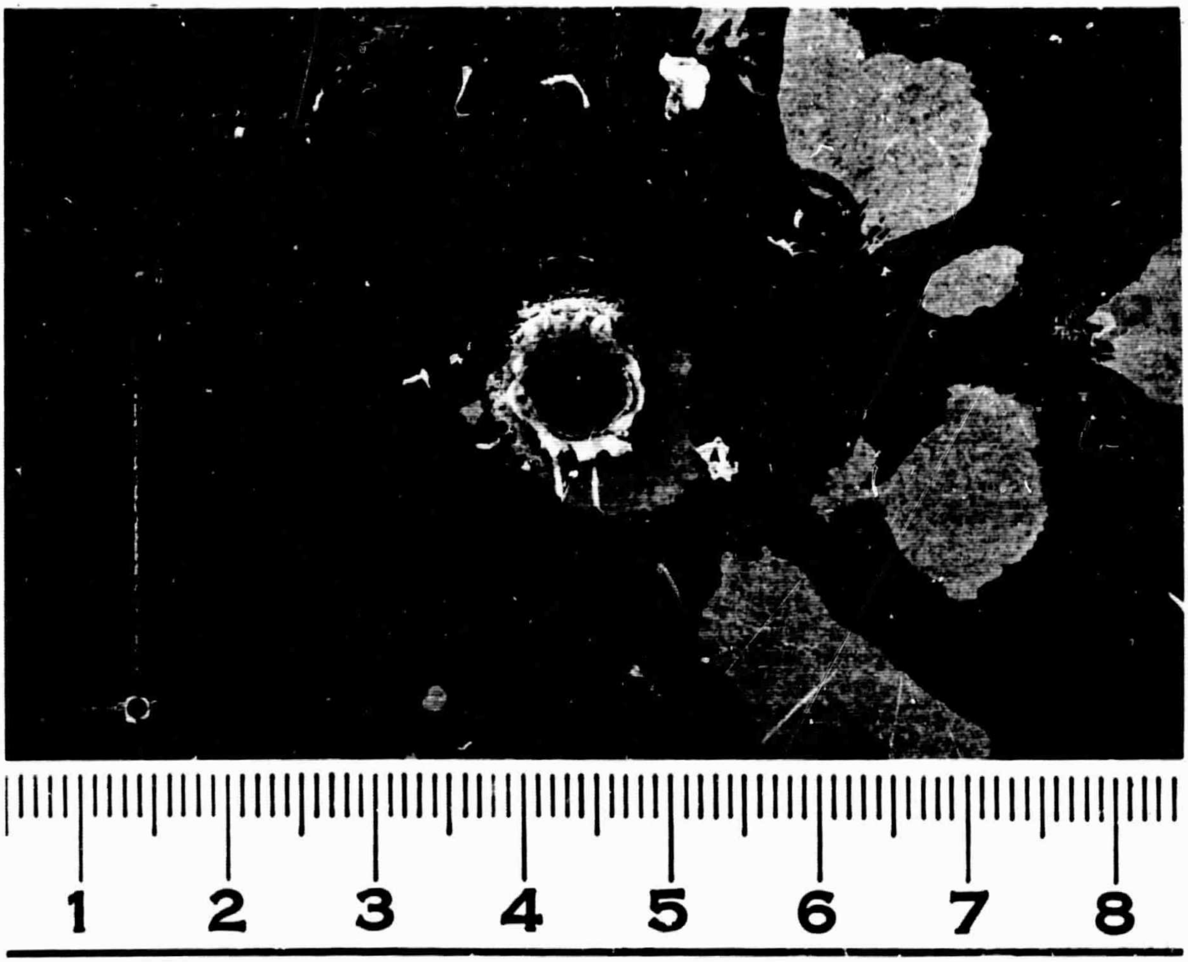

Figure 6 Crater produced by projectile in shot 1.7.

The results of the variation of the projectile position within the charge can be summarized in terms of the parameter k (see subsection 2.2) for constant drag acceleration. Figure 7 shows the variation of k with angular divergence and run-in distance. The trend of the two curves indicates that higher velocities can be expected with longer run-in distances; therefore, boundary layer growth was unimportant for these tests. Also, the angular divergence of the experiments was rather varied, one experiment (not shown on Figure 7) having a divergence of about 10 degrees.

Attempts were made to reduce the dispersion by variations in the charge initiation system and projectile suspension system. Charges were originally initiated uniformly around their circumference by an explosive train which was activated by a single detonator. This was changed to four detonators, simultaneously energized, directly initiating the Detatube charge. Projectiles were suspended by Mylar tape and magic mending tape. Later in the program, the projectile was taped to a very thin styrofoam disk which was inserted down the bore of the charge. None of these techniques reduced the dispersion.

In addition to dispersion, another nonideal effect observed during the program was the ablation of projectiles moving down the shot range. The framing camera record of a shot sometimes showed that a projectile "split" into two parts after emerging from the opaque accelerator gases. Each part followed the trajectory of the original projectile. This severe ablation can be seen very clearly in Figure 8, which shows three frames from the camera record of shot 1.10. The increased ablation rate is apparently due to a jump in the drag force on the projectile when it emerges from the accelerator gases. The drag force, which is a function of the relative velocity between projectile and surrounding gas, increases because the accelerator gases are moving

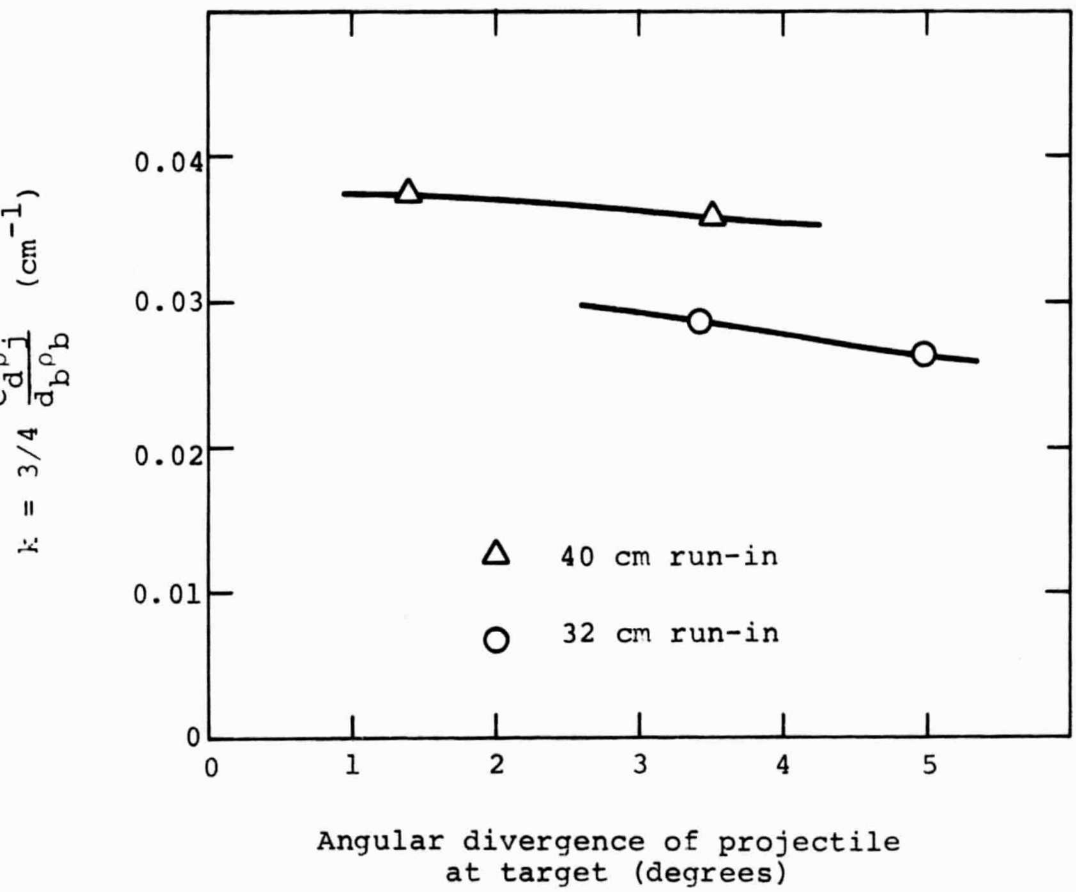

Figure 7 Variation of the constant drag acceleration parameter k with projectile divergence and run-in distance.

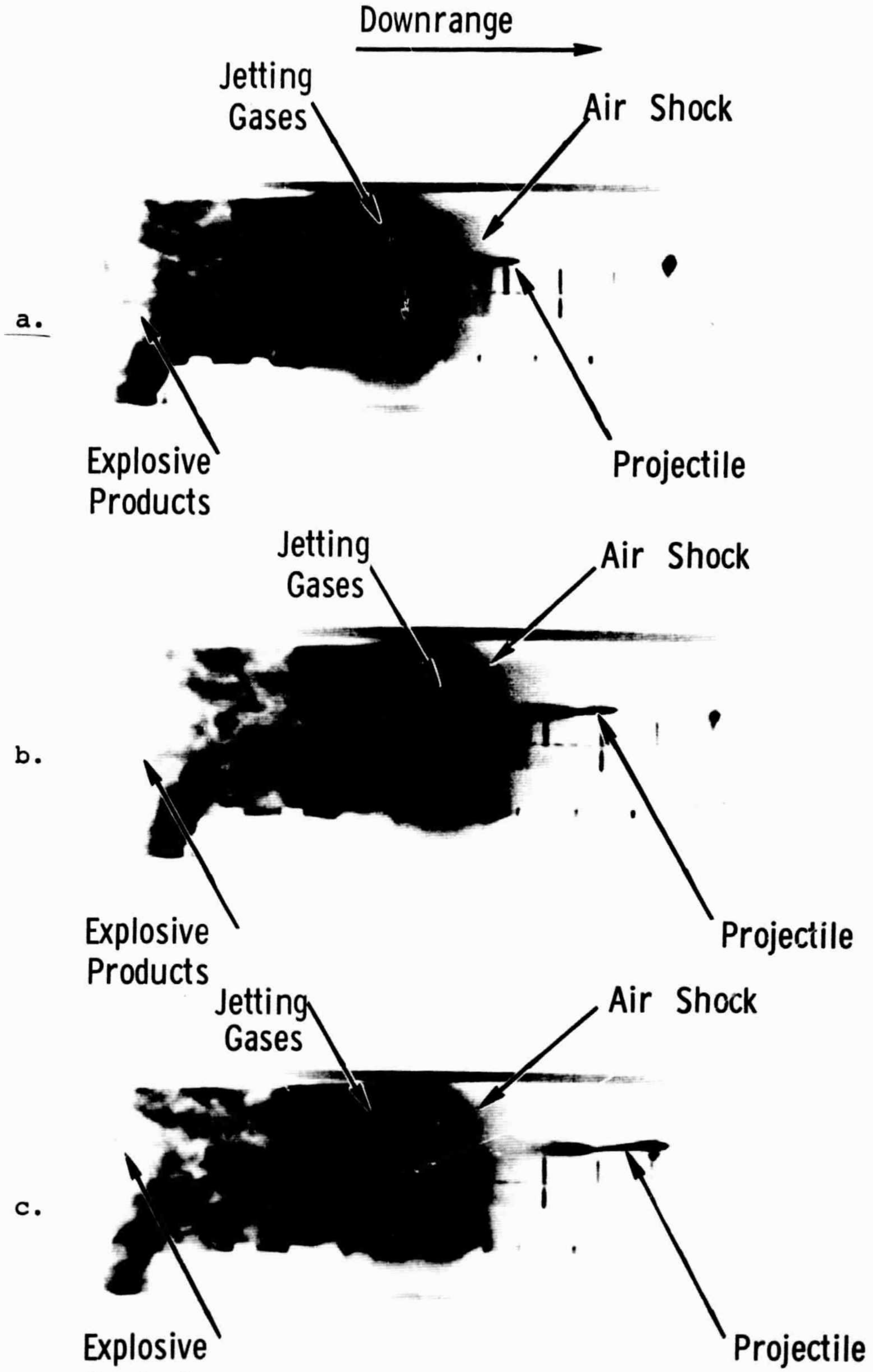

Figure 8 Sequence from framing camera record of shot 1.10 showing severe projectile ablation.

down range at several kilometers per second, while the ambient air is at rest. In addition, the projectile has been heated by the launch cycle and is more susceptible to ablation.

3.3 EXPERIMENTS 1.11 TO 1.13 - BOUNDARY LAYER STUDIES

The increase of k with run-in distance indicated that boundary layer growth was unimportant for the first ten tests, where the longest charge length was 48 cm, or 33 charge diameters. The objective of the next experiments was to investigate boundary layer growth in very long charges of Detatube and to obtain information on the gasdynamics of the jetting gases. A representative shot is 1.12, which was 150 cm long (or 100 charge diameters) and was fired in ambient air. Shorting ionization pins within the explosive monitored the arrival of the detonation wave, while ionization pins, pushed through the explosive into the jet, recorded the passage of the jet-driven air shock. The location of the contact surface between the cool, jetting explosive products and the hot, shocked air can be photographically recorded with a high-speed framing camera. To do this, a 15-cm-long Lucite extension was placed at the muzzle end of the charge to contain the emerging jet for photography. Finally, four projectiles were placed at the muzzle of the charge, with one on axis and three off axis. The three off-axis spheres were halfway between the axis and the charge inner wall, 120 degrees apart. The shot range was instrumented with range switches, a high-speed framing camera, and flash radiographs.

A distance-time plot of the data from 1.12 (see Figure 9) demonstrated that boundary layer effects were unimportant until 50 charge diameters in ambient air. Therefore, the factor limiting the acceleration path length and thus the performance of the

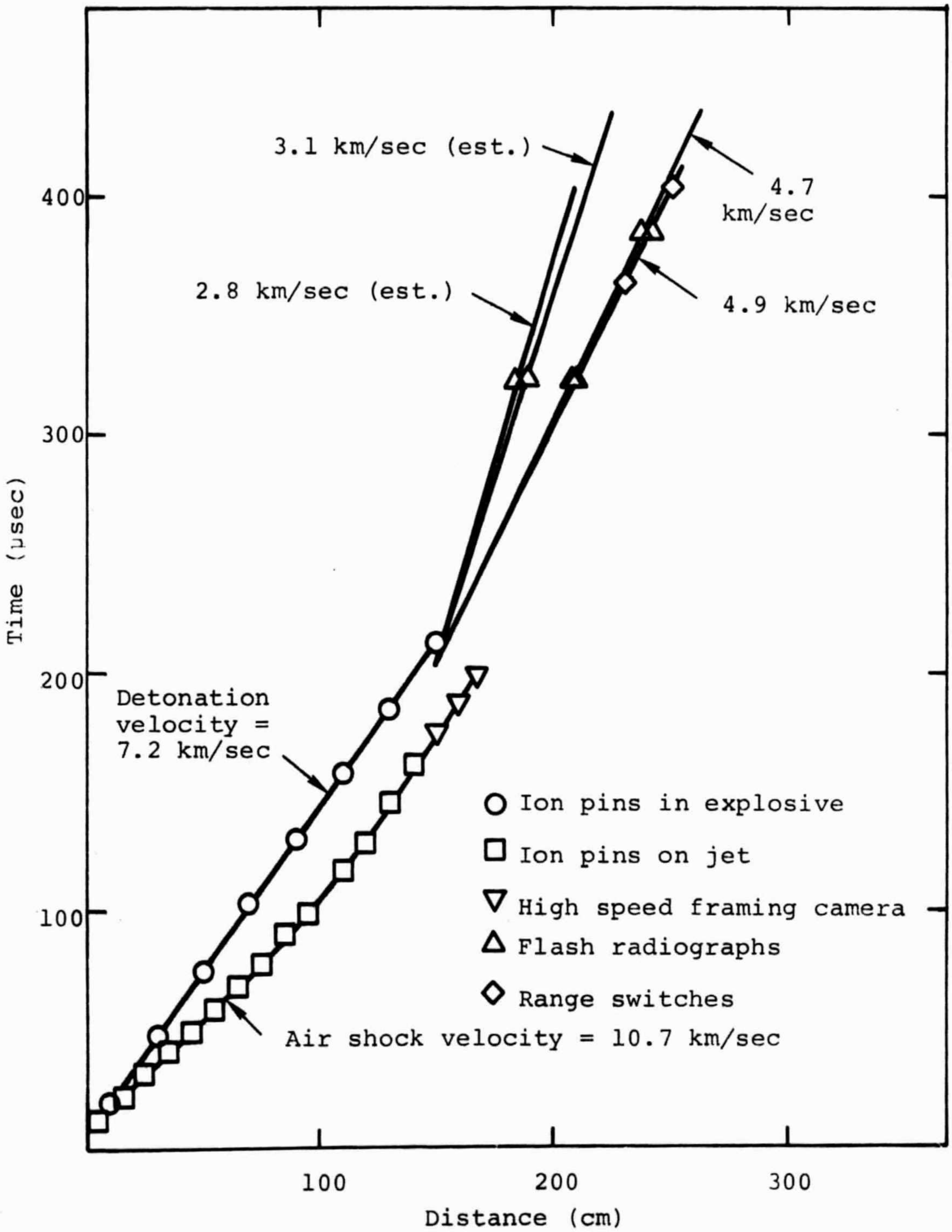

Figure 9 Distance - time plot for shot 1.12.

drag accelerator is not boundary layer but angular divergence. The four projectiles were not accelerated uniformly with respect to velocity (Figure 9) or angle, as can be seen from the target (Figure 10); this implies that the jet in Detatube is highly nonuniform.

The large angular dispersions and consequent lack of repeatability of the experiments appears to be due to the jet nonuniformities. A high-quality cast and machined explosive charge would probably improve the uniformity because the high dimensional tolerances and extremely constant planar detonation wave would produce very little perturbation to the jet formation process. Detatube, being extruded and coarse-grained, lacks dimensional control and has an inconstant detonation wave compared to an explosive such as HMX.

A similar experiment in helium at 14.7 psia produced higher shock velocities (12.1 km/sec as compared to 10.7 km/sec in air) and longer ideal operating lengths, with boundary layer effects absent until at least 75 charge diameters. The uncertainty is due to the weak ionization behind the helium shock adversely affecting ion pin response. Two of the projectiles emerged at 4.3 and 4.8 km/sec, corresponding to the velocities in air of 4.7 and 4.9 km/sec. This indicates that most of the projectile acceleration is performed by the jetting explosive gases and not the shocked air or helium. In other words, the projectile velocity appears to be independent of the ambient gas in the charge bore. On the basis of this conclusion, further work with a low-pressure air system does not appear likely to increase projectile velocities appreciably.

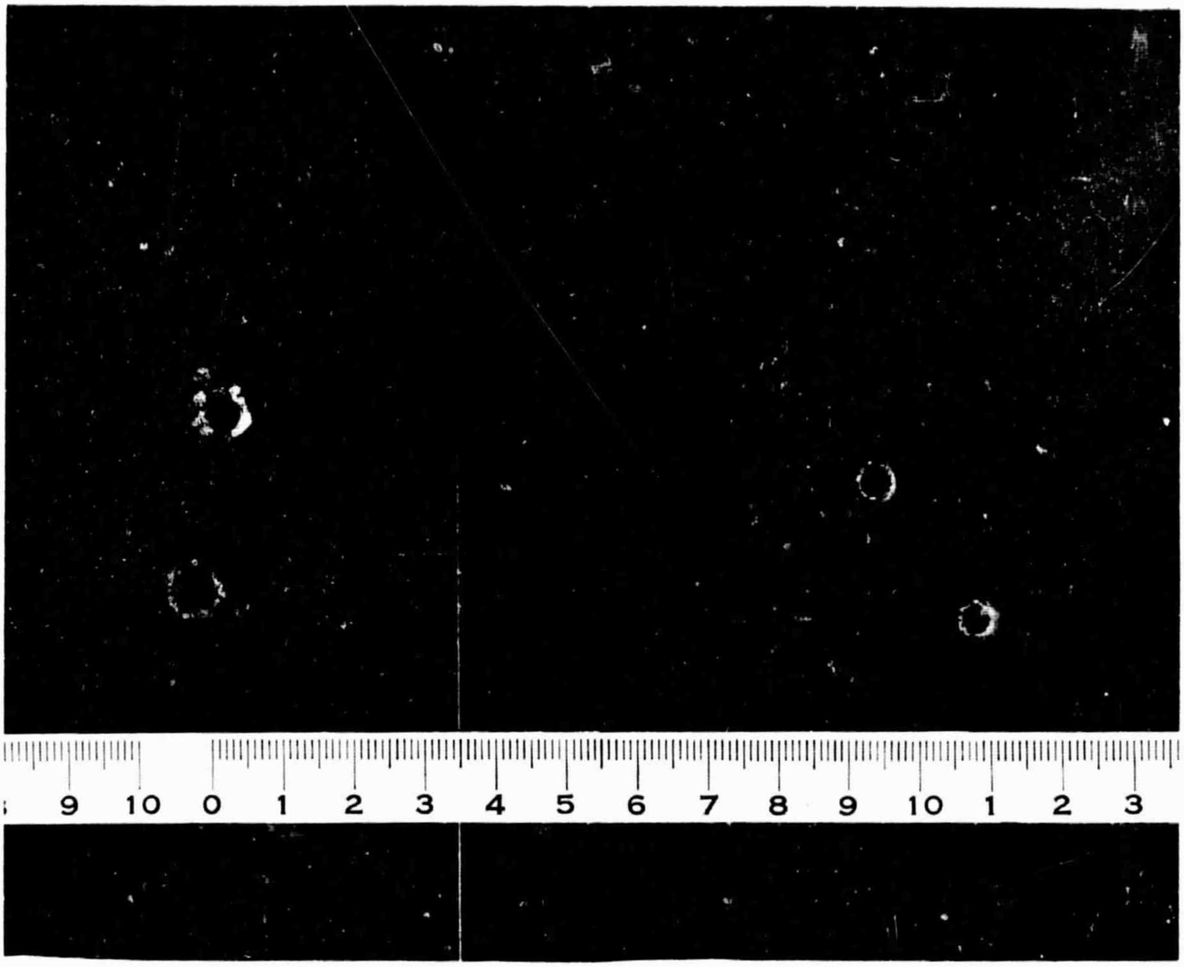

Figure 10 Target of shot 1.12 showing the differing velocities and dispersion of the four projectiles.

The responsibility of jetting explosive products for the projectile acceleration is supported theoretically by calculating the dynamic pressure, ρu^2, in the different regions of the jet. The dynamic pressure is the important variable because it is proportional to the drag force. The dynamic pressure of the explosive products is on the order of 10^{11} dyne/cm^2, while the dynamic pressure behind the air and helium shocks is approximately 10^{10} and 10^9 dyne/cm^2 respectively. Therefore, the drag forces differ by at least an order of magnitude between the explosive products and the shocked driver gas.

The air and helium shock velocities can be applied in various simplified one-dimensional theories to analyze the state of the jetting gases. The result of this effort is not consistent with the average jet density calculated by the method of subsection 2.2. The simplest explanation for this discrepancy is that the jet has a strong two-dimensional character. In particular, jet density must vary fairly sharply in the axial direction.

3.4 EXPERIMENTS 1.14 THROUGH 1.16 - VARIATION OF EXPLOSIVE MATERIAL

In order to vary the explosive material, charges of Composition C-4 were used. Composition C-4 has a detonation velocity of 8.0 km/sec and should produce higher velocity projectiles than Detatube for a comparable acceleration path. In addition, the angular dispersion might be reduced by careful preparation and packing of the charge. The instrumentation for this series of experiments was identical to that used for shots 1.3 to 1.10. The first experiment (shot 1.14), with a 40-cm run-in and an 8-cm acceleration path, produced a projectile traveling at 10.0 km/sec, measured by the high-speed framing camera record. The projectile, initially a 1.6-mm-diameter sphere of annealed 52100 steel, was ablated to approximately 50 percent of the original diameter and had an angular divergence of 4 degrees. A view of the projectile moving down the range as photographed by the framing camera is shown in Figure 11. A careful analysis of the framing camera record demonstrated that the projectile broke up during the launch cycle. This is shown by several very faint streaks which move down the range on different trajectories than the main projectile. These other particles have an extremely small mass since they do not appear on the flash radiographs and slow down very quickly. This form of projectile break-up is, however, a minor problem.

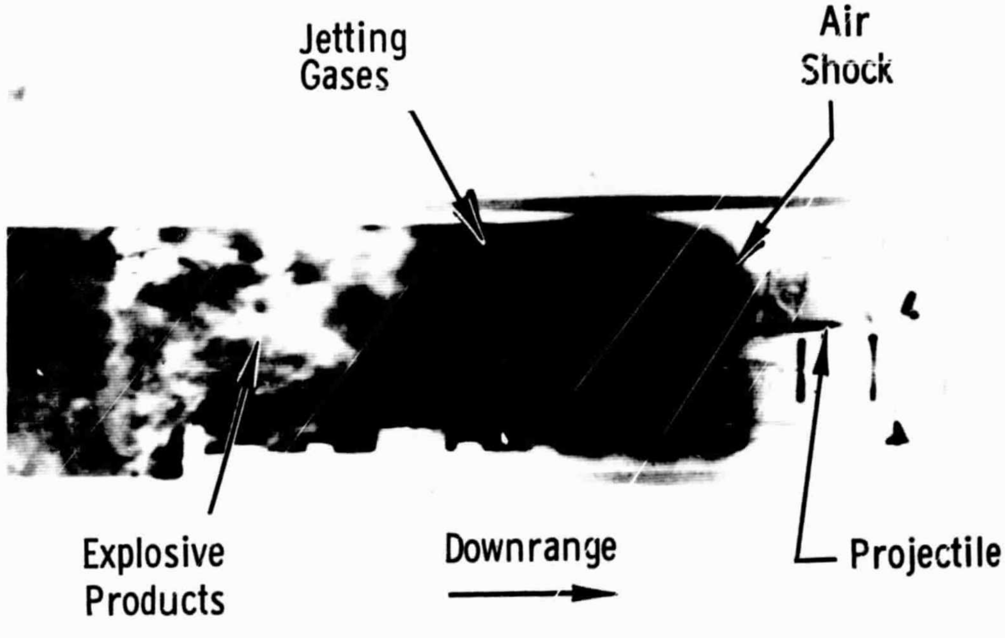

Figure 11 Framing camera record from shot 1.14.

The second test with C-4 had a longer acceleration path (12 cm) and significant projectile integrity problems. Multiple craters were produced by this shot, and the various projectile parts can be seen very clearly in the framing camera record (see Figure 12). Fragment velocities were between 9 and 10 km/sec.

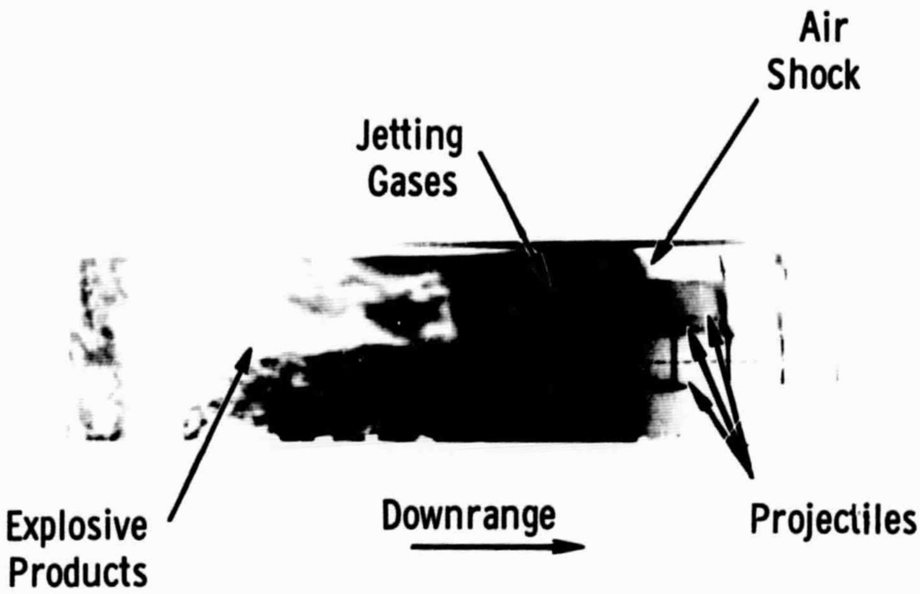

Figure 12 Framing camera record of shot 1.15. Projectile has broken up during the launch cycle.

As the environment of the C-4 accelerator appeared to be too severe for the annealed 52100 steel, a two-stage launcher was designed. The first stage used Detatube with a 40-cm run-in and an 8-cm acceleration path, joined to a 20-cm extension of packed C-4. No projectile emerged and it is thought that angular divergence caused the projectile to leave the main jetting gases, to slow down, and to be overtaken by the detonation wave.

3.5 EXPERIMENTS 1.17 THROUGH 1.19 - VARIATION OF C/A_j AND PROJECTILE DIAMETER

Rather than continue investigating a two-stage driver, a simple alternative method for reducing the initial loading on the projectile was to reduce the jet density. This can be accomplished by lowering the charge wall thickness, i.e., the parameter C/A_j, the ratio of the charge mass per unit length to jet area ratio. The elementary theory of subsection 2.1 indicates that the jet density is directly proportional to C/A_j for the fully expanded jet.

Shots 1.17 and 1.18 used C-4 explosive and had a C/A_j of 12.7 and 8.4, respectively. These values may be compared to experiment 1.14 with a C/A_j of 16.1. The configuration of these shots with respect to instrumentation, total charge length, and projectile position was identical to shot 1.14. The projectiles of neither shot maintained physical integrity. Each experiment had two craters in the target and two trails in the framing camera record.

Details of the projectile velocities and dispersions may be found in subsection 3.6. The predicted proportionality between C/A_j and the jet density was maintained between shots 1.14 and 1.17 but not for shot 1.18.

The final experiment in the program varied the projectile diameter with a 1-mm-diameter annealed 52100 steel sphere in a Detatube accelerator. The run-in and acceleration path were 40 cm and 8 cm, respectively, while instrumentation was identical with that of shots 1.3 through 1.10. Again the projectile broke up, producing two craters and a double trail on the framing camera record. This was the only time Detatube caused a projectile to break up in this way. This may have been caused by the projectile being accelerated through more projectile diameters within the explosive charge. This should produce more heating and a weaker projectile and could cause break up.

3.6 SUMMARY OF EXPERIMENTAL RESULTS

The following table presents the results of all experiments performed during this program. The purpose and instrumentation of each shot may be found in Appendix A. Unless otherwise noted, all projectiles were 1.6-mm diameter spheres, and all experiments were fired in ambient air.

The parameter k and jet density were calculated by the method outlined in subsection 2.2, where a jet velocity equal to twice the detonation velocity has been assumed. Thus, jet velocities were 14.2 km/sec and 16.1 km/sec for Detatube and C-4, respectively. The average jet density for shots using Detatube is 0.06 gram/cc, quite close to the published Russian result of 0.0605 gram/cc. Experiments with C-4 yielded higher jet densities due to the severe projectile ablation and break up, requiring an effective projectile diameter to be used in the calculations. No attempt was made to take this into account.

RESULTS OF EXPERIMENTAL PROGRAM

Shot Number	Explosive	Run-in Distance (cm)	Acceleration Path (cm)	Projectile Material	Projectile Velocity (km/sec)	Angular Divergence (degrees)	k (cm^{-1})	Jet Density (gram/cc)	Notes
1.1	Detatube Type 1	32	8	Hardened 52100 steel					Rectangular geometry did not jet.
1.2	Detatube Type 1	35	8	Hardened 410 stainless steel					Fired in 12 torr air; no projectile emerged.
1.3	Detatube Type 1	32	8	Hardened 410 stainless steel					Projectile broke up.
1.4	Detatube Type 1	32	8	Hardened 52100 steel	6.3	4.96	0.0264	0.0482	
1.5	Detatube Type 1	32	12	Hardened 52100 steel					No projectile emerged; overrun by the detonation.
1.6	Detatube Type 1	32	4	Hardened 52100 steel	5.1	3.42	0.0288	0.0525	
1.7	Detatube Type 1	32	8	Annealed 52100 steel	6.95	1.96	0.0358	0.0654	
1.8	Detatube Type 1	40	4	Annealed 52100 steel	5.6	1.38	0.0373	0.0680	
1.9	Detatube Type 1	40	8	Annealed 52100 steel	5.7	~10	0.0196	0.0358	
1.10	Detatube Type 1	40	8	Annealed 52100 steel	6.95	3.50	0.0358	0.0654	Repetition of 1.9 because of large divergence.
1.11	Detatube Type 1	75	0	Annealed 52100 steel	3.2	2.84			Boundary layer shot, 50 charge diameters; projectile at charge muzzle.
1.12	Detatube Type 1	[illegible]	15[1]	Annealed 52100 steel	4.9 4.7 3.1 2.8	2.15 2.20 3.42 4.56			Boundary layer shot, 100 charge diameters; 4 projectiles at muzzle.

RESULTS OF EXPERIMENTAL PROGRAM (Cont')

Shot Number	Explosive	Run-in Distance (cm)	Acceleration Path (cm)	Projectile Material	Projectile Velocity (km/sec)	Angular Divergence	k (cm^{-1})	Jet Density (gram/cc)	Notes
1.13	Detatube Type 1	150	15[1]	Annealed 52100 steel	4.85 4.3 <3.8 <3.8	4.08° 4.62° 4.44° 1.92°			Boundary layer shot, 100 charge diameters, helium atmosphere, 4 projectiles at muzzle.
1.14	Composition C-4	40	8	Annealed 52100 steel	10.0	3.94°	0.0837	0.153	C/A_j = 16.1 gram/cm^2
1.15	Composition C-4	40	12	Annealed 52100 steel	9.5 9.7 9.7	Not on target 7.5° 1.72°	0.0492 0.0492	0.0897 0.0897	Projectile broke up.
1.16	Detatube - C-4	40	8 plus 20[2]	Annealed 52100 steel					Two-stage driver; no projectile emerged.
1.17	Composition C-4	40	8	Annealed 52100 steel	9.4 9.25	3.65° 4.0°	0.0656 0.0620	0.120 0.113	C/A_j = 12.72; projectile broke up.
1.18	Composition C-4	40	8	Annealed 52100 steel	7.6 7.6	5.44° 5.11°	0.0319	0.0582	C/A_j = 8.35; projectile broke up.
1.19	Detatube Type 1	40	8	Annealed 52100 steel	7.4 7.25	7.1° 5.26°	0.0441	0.0506	1.0-mm-diameter projectile. Projectile broke up.

[1] Fifteen-cm Lucite extension at muzzle end of accelerator for photography.

[2] Detatube first stage with a 40-cm run-in and an 8-cm acceleration path, plus a 20-cm-long second stage of C-4.

SECTION 4

CONCLUSIONS AND RECOMMENDATIONS

The basic operating parameters affecting the performance of the explosive hypervelocity drag accelerator were varied during this program. Important theoretical and experimental results were:

a. Projectile velocity depended upon run-in distance as well as the acceleration path and angular divergence, with velocity increasing with increasing run-in distance.

b. Projectile material properties are critical, ductility probably being as important as hardness and strength for a steel sphere.

c. The average jet density calculated from experiments 1.3 through 1.10 was within several percent of the value determined by the Russian investigators.

d. Boundary layer effects are unimportant for accelerators up to 50 charge diameters in length. Standard accelerators during the program were less than 40 diameters in length.

e. The jet of a Detatube charge was found to be highly unsymmetric across a given cross section.

f. Simplified one-dimensional analysis of the gasdynamics of the jet failed to give results compatible with a jet density calculated as outlined in subsection 2.2.

g. The angular divergence of the projectiles was not reduced by a variety of projectile suspension techniques and explosive initiation methods.

h. The maximum velocity achieved was 10 km/sec.

The drag accelerator appears capable of higher velocities than 10 km/sec with further development. Additional work is necessary to find an improved projectile material and to reduce angular dispersion. The Russians claim to have successfully solved these two problems, and it seems probably that the material properties difficulties can be overcome by testing a wide variety of steels. A cast and machined, high-quality explosive should be tested to attempt to improve the uniformity of the jet and to reduce the angular dispersion.

REFERENCES

1. V. M. Titov, Yu. I. Fadayenko, and N. S. Titova, "Acceleration of Solid Particles by a Cumulative Explosion," Letters of the Academy of Sciences, USSR No. 5, Vol. 180, 1050-1052 (1968) (In Russian).

2. A. S. Zumennov, N. S. Titova, Yu. I. Fadeyenko, and V. P. Christyakov, "Detonation of Elongated Tubular Charges," Applied Mechanics and Technical Physics, (PMTF) No. 2, 79-82 (1969) (In Russian).

3. M. M. Rusakov, "Experimental Simulation of Meteoric Impingement," PMTF, No. 4, 167-169 (1969) (In Russian).

4. M. M. Rusakov, and M. A. Lebedev, "Determination of the Reaction Impulse in Experimental Modeling of Meteoric Impact," Kosmichcheskize Issledovaniya, Vol. 6, No. 4, 634 (1968) (In Russian).

5. M. A. Lavrentyev, "Cumulative Explosive Charge and Its Operating Principle," (Kumyliativnyy Zaryad i print sipy ego raboty) Uspekhi Matematickes kikh Nauk, Vol 12, No. 4 (76), 41-56 (1957).

6. N. I. Novikov, "Some Properties of High Velocity Cumulative Jets," Zhurnal Prikladnoi Mekhaniki i Tekhmcheskoi Fiziki, No. 1, 3-13 (1963).

APPENDIX A

The following table presents a summary of the purpose and instrumentation of each experiment in this program. The code for the instrumentation is:

X - flash radiographs

RS - shorting range switches and target

FC - high-speed framing camera

SC - streaking camera

I - shorting ionization pins in the explosive charge

The preliminary drag accelerator experiment, mentioned in the table, was performed prior to this program on in-house funding. The preliminary shot was identical to shot 1.4.

PURPOSE AND INSTRUMENTATION ON SHOTS 1.1 THROUGH 1.19

EXPERIMENT NO.	INSTRUMENTATION	PURPOSE	RESULT
1.1	X; RS; FC; SC; I	Variation of explosive geometry to determine the performance of a rectangular accelerator.	Rectangular geometry did not jet.
1.2	X; RS; I	Test of the effect of low pressure air in the charge bore.	Nc projectile emerged.
1.3	X; RS; FC; SC; I	Variation of projectile material; repetition of the preliminary drag accelerator shot with a hardened 410 stainless steel projectile.	Projectile broke up.
1.4	X; RS; FC; I	Variation of projectile material; repetition of shot 1.3 with a hardened 52100 steel projectile.	Successful shot.
1.5	X; RS; FC; I	Variation of acceleration path length; path increased 4 cm over shot 1.4.	No projectile emerged.
1.6	X; RS; FC; I	Variation of acceleration path length; path decreased 4 cm from shot 1.4.	Successful shot.
1.7	X; RS; FC; I	Variation of projectile material; projectile made of annealed 52100 steel; same configuration as shot 1.4.	Successful shot.
1.8	X; RS; FC; I	Variation of run-in distance; run-in 8 cm longer than shot 1.6.	Successful shot.
1.9	X; RS; FC; I	Variation of run-in distance; run-in 8 cm longer than shot 1.4.	Projectile emerged, but with a large angular divergence.
1.10	X; RS; FC; I	Repetition of 1.9 because of large dispersion.	Successful shot.
1.11	X; RS; I	Study of boundary layer growth and the gasdynamics of the jet; charge length 50 charge diameters.	No boundary layer effects were observed at 50 diameters.
1.12	X; RS; FC; I	Repetition of shot 1.11 with a charge length of 100 diameters.	Successful shot.
1.13	X; RS; FC; I	Repetition of shot 1.12 with helium at 14.7 psia in the charge bore.	Successful shot.

PURPOSE AND INSTRUMENTATION ON SHOTS 1.1 THROUGH 1.19 (Cont')

EXPERIMENT NO.	INSTRUMENTATION	PURPOSE	RESULT
1.14	X; RS; FC; I	Variation of explosive material; charge made of packed Composition C-4; same charge configuration as shot 1.10.	Successful shot.
1.15	X; RS; FC; I	Variation of acceleration path; repeat of 1.14 with the acceleration path increased by 4 cm.	Projectile broke up.
1.16	X; RS; FC; I	Variation of explosive configuration; two-stage accelerator for a soft launch.	No projectile emerged.
1.17	X; RS; FC; I	Variation of explosive geometry; repetition of shot 1.14 with a lower C/A_j (charge mass per unit length to jet area ratio).	Projectile broke up.
1.18	X; RS; FC; I	Variation of explosive geometry; shot fired with a lower C/A_j than shot 1.17.	Projectile broke up.
1.19	X; RS; FC; I	Variation of projectile diameter; repetition of 1.10 with a smaller diameter projectile.	Projectile broke up.